Techno-economic versus Energy Optimization of Natural Gas Liquefaction Processes with different Heat Exchanger Technologies

Heechang Son [a], Bjørn Austbø [b, *], Truls Gundersen [b], Jihyun Hwang [c], Youngsub Lim [a, d **]

[a] *Department of Naval Architecture and Ocean Engineering, Seoul National University, Seoul, 08826, Republic of Korea*

[b] *Department of Energy and Process Engineering, Norwegian University of Science and Technology (NTNU), NO-7491 Trondheim, Norway*

[c] *School of Energy Technology, Korea Institute of Energy Technology, Naju, 58330, Republic of Korea*

[d] *Research Institute of Marine Systems Engineering, Seoul National University, Seoul 08826, Republic of Korea*

[*] Corresponding author. *E-mail address:* bjorn.austbo@ntnu.no

[**] Corresponding author. *E-mail address:* s98thesb@snu.ac.kr

Keywords:

Natural gas liquefaction process

Techno-economic optimization

Energy optimization

Main cryogenic heat exchanger

Minimum temperature approach

Abstract

The energy intensity of the natural gas liquefaction process in LNG value chains is considerable, and therefore a number of energy optimization studies to obtain optimal operating conditions and maximize process efficiency. In order to limit the size and cost of heat exchangers during energy optimization, a minimum temperature approach constraint is used for heat exchangers, primarily as an economic trade-off parameter. However, the cost optimal solution and appropriate values for the minimum temperature approach constraints depend on the process concept and the heat exchanger type. In this study, techno-economic optimization and energy optimization are performed for three different natural gas liquefaction processes and two different heat exchanger types with different unit cost and heat transfer performance. The results indicate that the techno-economic optimization can provide a better distribution of temperature driving forces in the heat exchangers and thereby lower total annualized cost

irrespective of the minimum temperature approach constraint. The energy optimization performs better for low-efficiency processes than high-efficiency processes in terms of the total annualized cost. In addition, based on the techno-economic optimization results, appropriate values for the minimum temperature approach constraints as economic trade-off parameters in the energy optimization are investigated for the two heat exchanger types.

1. Introduction

Owing to global warming and particulate emissions, the demand for eco-friendly natural gas and liquefied natural gas (LNG), which are cleaner fossil fuels than coal and oil [1, 2], is gradually increasing [3, 4]. The total energy share of natural gas is predicted to increase from 20% in 2017 to 25% in 2040, making it the second largest source of energy following oil [5]. Trading of LNG is also expected to increase to cover 20% of the world's natural gas needs by 2040 because of the increase in its supply and the shale gas market in North America that continues to expand [5, 6].

The liquefaction process for natural gas is a key process for LNG production given the large energy requirements for cooling natural gas to obtain LNG. Natural gas must be cooled to cryogenic conditions ($< -160\,℃$) at atmospheric pressure to produce LNG. Therefore, the energy efficiency of the liquefaction process is important for the economic viability of LNG.

Because of the above-mentioned characteristics, many previous studies on natural gas liquefaction processes have focused on minimizing the energy requirements. Energy-based studies aimed at minimizing power consumption can typically be divided into three categories: (1) application of optimization algorithms, (2) advanced configuration development, and (3) exergy analysis.

It is important to determine the operating conditions that maximize the process efficiency, which can be achieved using an optimization algorithm [7]. Various optimization algorithms have been applied in previous studies to determine the optimal operating conditions and minimize the power consumption. Wahl et al. [8] performed energy optimization for the PRICO process using sequential quadratic

programming (SQP). With the use of SQP, the optimal solution was identified faster than by Aspelund et al. [9], who performed optimization using Tabu Search (TS) and the Nelder–Mead Downhill Simplex (NMDS) method. It was confirmed that the performance of SQP is good for simple processes; nonetheless, it is difficult to achieve good performance for complex processes. Owing to its characteristics such as tight heat transfer conditions, the liquefaction process requires rigorous and complex thermodynamic models. Gradient-based optimization methods can suffer from the complexity of these models.

Morin et al. [10] performed energy optimization by applying an evolutionary search to overcome the shortcomings of local optimization algorithms such as SQP. It was shown that optimization using evolutionary search obtained robust optimal solutions, even for a complex process. Alabdulkarem et al. [11] optimized a propane precooled mixed refrigerant (C_3MR) LNG plant using a genetic algorithm (GA), and the total power consumption was reduced by 9.1% compared to a base case by Mortazavi et al. [12]. Shirazi and Mowla [13] performed energy optimization by applying GA to a single mixed refrigerant (SMR) process in a peak-shaving plant and obtained energy savings of 3.0–6.5% compared to those of previous studies. Hwang et al. [14] performed energy optimization for a dual mixed refrigerant (DMR) process using a hybrid optimization method that consisted of GA and SQP, resulting in a reduction in energy use by 34.5% compared to a patented process [15] and by 1.2% compared to that of a previous study [16]. Wang et al. [17] developed a synthesis model with regressed thermodynamic properties and solved the resulting mixed-integer non-linear programming (MINLP) problem using the LINDOGlobal solver in GAMS. The methodology was applied to a C_3MR process, resulting in 13.0% reduction in energy use compared to the base case. Khan et al. [18] proposed and applied a knowledge-based optimization approach to SMR and C_3MR processes to increase the process efficiency. As a result, the power consumption of the SMR and C_3MR processes was reduced by 30% and 13%, respectively, compared to base cases.

As previously mentioned, the process efficiency can also be improved by advancing the configuration of the process. For example, He and Ju [19] optimized four configurations based on expansion cycles

for liquefaction in a small-scale LNG plant and found that a configuration with R410A precooling and parallel nitrogen expansion cycles achieved the best performance. Qyyum et al. [20] proposed a C_3–N_2 two-stage expander cycle, and the power consumption was reduced by 46.4% compared to that of the conventional N_2 single expander cycle. Chang et al. [21] proposed an N_2-C_2-C_3 cycle to increase the process efficiency of the expander cycle. Qyyum et al. [22] suggested a dual-effect single-mixed refrigeration cycle to compensate for the limitations (such as process complexity and high sensitivity to operating conditions) of the DMR process. Wang et al. [1] suggested a C_3&C_4-MR liquefaction process that uses propane and isobutane as pre-coolants to reduce the power consumption of the process.

In addition, there are studies related to exergy analysis that highlight the possibility of efficiency improvement. Kanoglu et al. [23] provided an exergy analysis of a multistage cascade refrigeration cycle. Venkatarathnam and Timmerhaus [16] performed design and exergy analysis for various liquefaction processes. Remeljej and Hoadley [24] conducted exergy analyses of four different LNG processes for small-scale plants. Primabudi [25] performed exergy and exergoeconomic analyses for a C_3MR process to determine key design variables, and then optimized the process using GA.

Relying on the above energy-based studies, it is possible to reduce the operating cost of the liquefaction processes by reducing power consumption. However, focusing only on the improvement of the process efficiency can impair other important factors. For example, it can lead to an increase in the size and capital cost of the main cryogenic heat exchanger (MCHE). To prevent this issue, a minimum temperature approach (*MTA*) constraint is commonly used as an economic trade-off parameter when performing energy optimization. Depending on the selected value for the *MTA* constraint, energy optimization results can be significantly affected, and therefore selecting an appropriate value for the *MTA* constraint is important from an economic point of view when optimizing the liquefaction process.

Because the natural gas liquefaction process is responsible for a high proportion of the capital cost of the LNG value chain [22, 26], solutions that are more economical can be obtained if the capital cost is considered in addition to the operating cost. Although it is not easy to accurately estimate the capital cost [27], several researchers have attempted to consider the capital cost of liquefaction processes.

Barnés and King [28] estimated the cost of equipment by using equipment cost factors. Del Nogal et al. [29] optimized the design of a mixed refrigerant cycle considering the cost of heat exchangers. Jensen and Skogestad [30] argued that minimizing the power consumption of a liquefaction process with a *MTA* constraint for the MCHE may lead to suboptimal operating points and performed cost optimization considering both capital and operating costs by introducing a simplified total annualized cost (TAC) method. Hatcher et al. [31] performed optimization considering operation and design objectives with eight different objective functions, one of which was the net present value (NPV) that considers both the operating cost and capital expenditure. From a design perspective, the best results were obtained with NPV as the objective function. Wang et al. [32] proposed four different objective functions (total shaft work consumption, total cost investment, total annualized cost and total capital cost of compressors and MCHEs) and found that minimizing total capital cost of compressors and MCHEs was most appropriate to reduce both shaft work and heat exchanger area, which are two key variables of the total investment cost. Zhang et al. [33] performed energy and techno-economic optimization for expander-based processes in small-scale applications, resulting in reduced power consumption and production cost (which is the sum of amortized capital and operating costs required to produce 1 kg LNG).

There are various types of MCHEs that can be applied, and the characteristics of MCHEs can be significantly different depending on the type. For instance, both plate-fin heat exchangers and spiral-wound heat exchangers have been used as MCHEs in natural gas liquefaction processes, and these heat exchangers have different characteristics in terms of operating conditions and costs. Thus, the choice of the MCHE can affect the optimization results.

The novelty of this study is to examine the effects of different types of MCHEs for different natural gas liquefaction processes, both simple, less energy efficient processes and complex, more energy efficiency processes by performing energy optimization and techno-economic optimization. Here, two types of MCHEs with different heat transfer performance and unit cost are applied for the economic analysis. The manuscript provides insight into when the energy-based formulations perform better or worse based

on the techno-economic optimization results. This work also shows how the value of the *MTA* constraint affects the economy and how the optimal value for the *MTA* constraint during energy optimization (providing the smallest cost from energy optimization) changes with process type and equipment cost.

2. Process Description and Simulation

In this study, three liquefaction processes (N_2-C_1 dual expander, SMR and DMR) were selected to apply and compare energy optimization and techno-economic optimization. The processes can be divided into less efficient processes and more efficient processes due to their own characteristics, and were selected to understand the relationship between energy performance and economic performance. The selected N_2-C_1 dual expander, SMR, and DMR liquefaction processes from Venkatarathnam and Timmerhaus [16], as illustrated in Figures 1–3, were modeled and simulated using Aspen HYSYS® V10.0. In the figures, C, E, IC, VLV, V and MCHE stand for compressor, expander, intercooler, JT valve, vessel and main cryogenic heat exchanger, respectively. The Peng-Robinson equation of state, which is widely used in the oil and gas industries, was used to calculate the thermodynamic properties and phase equilibria [34]. The natural gas feed conditions and process parameters were set using the reference data shown in Tables 1 and 2, respectively [16, 35].

2.1. Dual expander process

The expander process, or reverse Brayton cycle, is a liquefaction cycle that has mainly been applied to small-scale LNG plants [19, 36, 37]. The expander process mainly uses non-flammable N_2 as a refrigerant, making it safe to operate. The refrigerant in the expander process is in gas phase for the entire cycle. Furthermore, the expander process is more compact than other processes and has advantages when exposed to motion on offshore platforms operated in a marine environment [38]. Because the process efficiency of a single expander process is quite low, with a specific energy consumption (SEC) of approximately 0.7–0.8 kWh/kg LNG [39], a dual expander process with two

expansion stages has been developed to counteract the limitation of single expander processes. The SEC of a dual expander process is about 0.5 kWh/kg LNG [39].

Dual expander processes often use two different refrigerant cycles instead of only N_2 refrigerant to further improve process efficiency. The dual expander process selected in this study consists of two cycles; one with N_2 as the refrigerant and the other with C_1 as the refrigerant, as illustrated in Figure 1. The main equipment of the dual expander process are the compressors, expanders, coolers (intercoolers), and the MCHE. Considering the compression ratio for the cycles, four compressor stages with intercoolers were installed in the N_2 refrigerant cycle whereas three compressor stages with intercoolers were installed in the C_1 refrigerant cycle.

2.2. SMR process

The SMR process uses a mixed refrigerant (MR) cycle to obtain higher efficiency than that of the expander processes. The SMR process is simple, and has been widely applied to small- and middle-scale LNG plants [37]. For an SMR process, the composition of the refrigerant has a dominant effect on the irreversibility of the MCHE and thereby the process performance [40, 41]. Therefore, it is important to select the optimal composition of the refrigerant when designing the SMR process. The MR typically consists of a combination of nitrogen and hydrocarbons [41, 42].

The simulated SMR process has compressors, JT valves, coolers (intercoolers) and the MCHE as the main equipment, as illustrated in Figure 2. After the compressed MR is cooled through the MCHE, it expands through a JT valve to reduce the temperature. In this work, the components of the refrigerant are nitrogen (N_2), methane (C_1), ethane (C_2), propane (C_3), normal butane (*n*-C_4), and isopentane (*i*-C_5). Considering the compression ratio for the cycle, two compressor stages with intercoolers were installed in the MR cycle.

2.3. DMR process

The DMR process was introduced to improve the SMR process by adding a precooling cycle and thereby use two MR cycles. With these characteristics, the DMR process has the highest energy efficiency of the three processes studied. However, the DMR process has a relatively large number of units, and its operation is difficult and sensitive, owing to its complex configuration. The MR of the precooling cycle (Warm Mixed Refrigerant – WMR) is composed of heavier components such as C_2, C_3 and C_4, whereas the MR of the main cryogenic cycle (Cold Mixed Refrigerant – CMR) is composed of lighter components such as N_2, C_1, C_2 and C_3 [37].

The CMR and the natural gas (NG) are cooled by the WMR to −33.15 °C during the precooling cycle, and then cooled to −160.1 °C through the main cryogenic cycle. Here, the components of the precooling cycle are C_2, C_3 and *n*-C_4, whereas the components of the main cryogenic cycle are N_2, C_1, C_2 and C_3. The compressors of the precooling cycle and the main cryogenic cycle were divided into two and three stages with intercoolers, respectively.

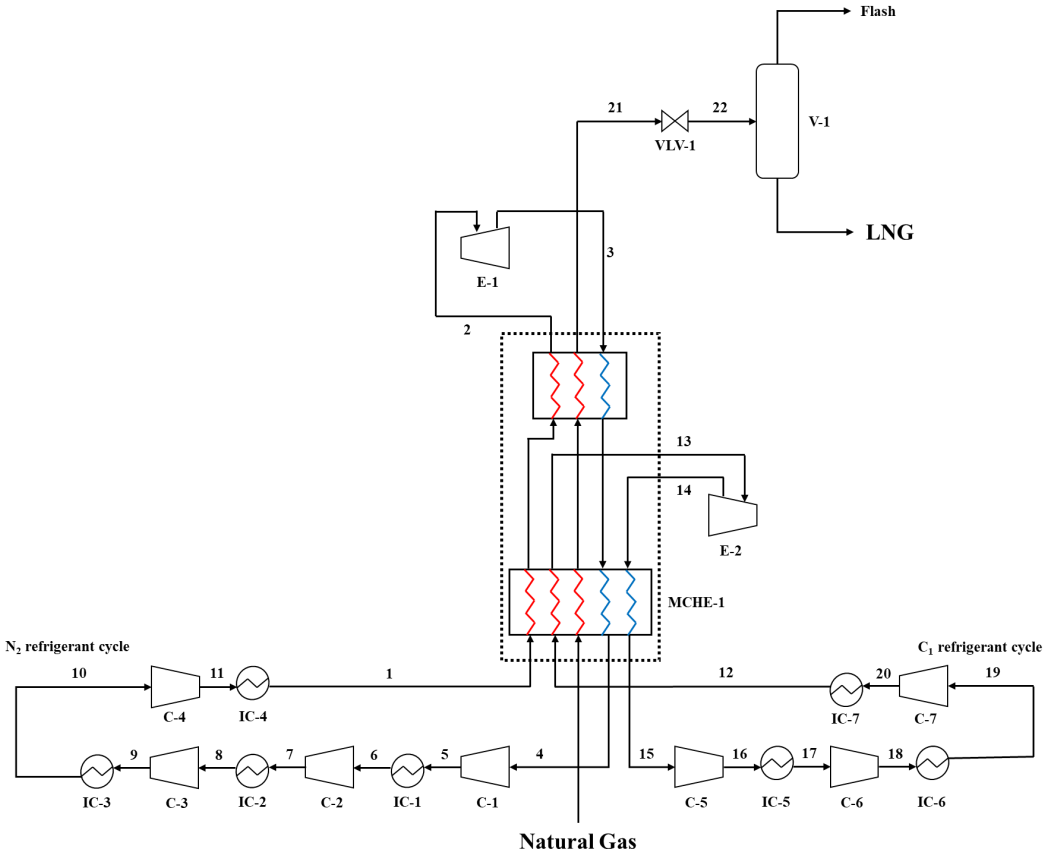

Figure 1. Process flow diagram of the dual expander process [16]

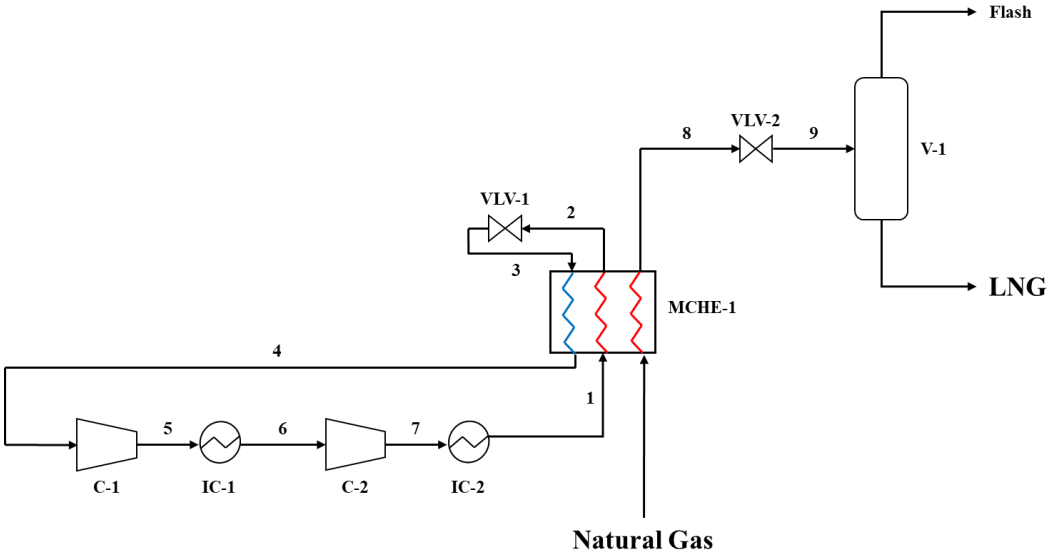

Figure 2. Process flow diagram of the SMR process [16]

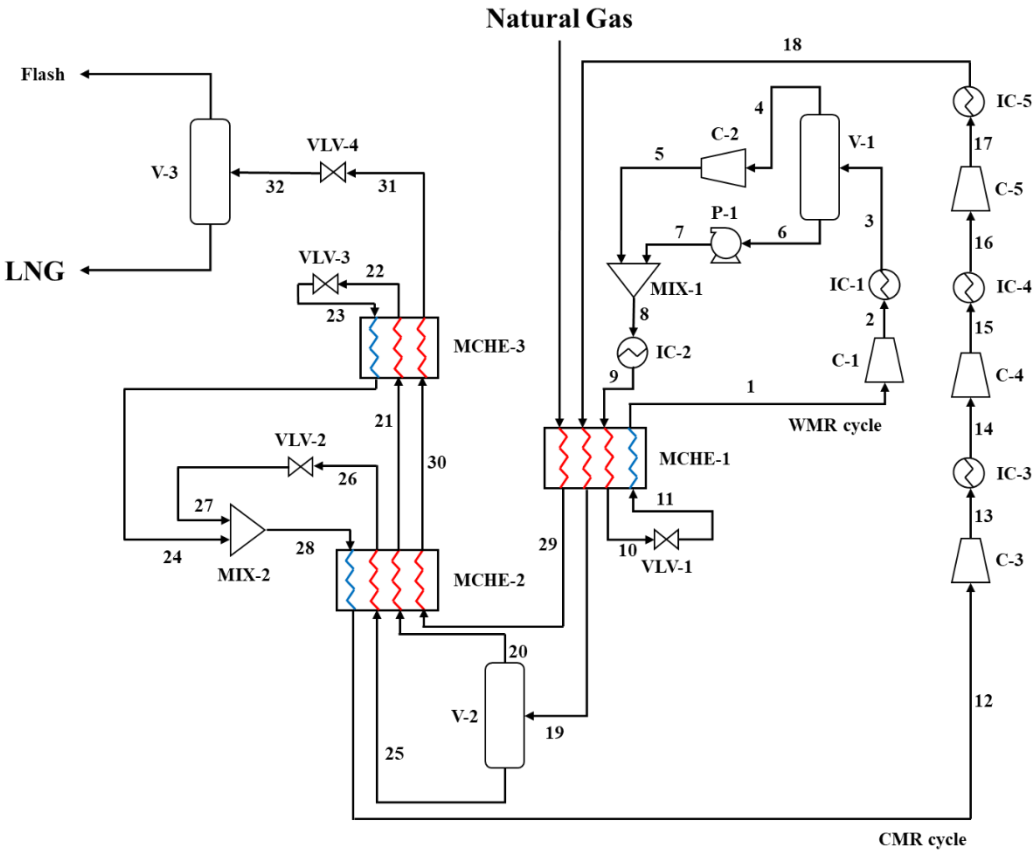

Figure 3. Process flow diagram of the DMR process [16]

Table 1. Natural gas composition [16, 35]

Component	Composition (mol %)
Nitrogen (N_2)	4.0
Methane (C_1)	87.5
Ethane (C_2)	5.5
Propane (C_3)	2.1
i-Butane (*i*-C_4)	0.3
n-Butane (*n*-C_4)	0.5
i-Pentane (*i*-C_5)	0.1

Table 2. Process parameters for simulation [16]

Parameter (Stream name or number)	Value

Pressure of natural gas feed stream (Natural Gas)	65 bar
Temperature of natural gas feed stream (Natural Gas)	26.85 °C
Flow rate of LNG stream (LNG)	18.22 ton/h
Pressure of LNG stream (LNG)	1.013 bar
LNG temperature before JT expansion (21, 8 and 31 in Figures 1, 2 and 3 respectively)	−160.1 °C
Pressure drop in the heat exchangers	0 bar
Refrigerant temperature leaving intercoolers	26.85 °C
Isentropic efficiency of compressors and expanders	80%

3. Optimization of natural gas liquefaction processes

For optimization, a genetic algorithm (GA) [43] was used in MATLAB R2020a. To execute the search, MATLAB loads the thermodynamic properties calculated by Aspen HYSYS®. The optimization algorithm uses the results from the Aspen HYSYS® simulation to perform a fitness evaluation and update the optimization variables. Here, if the output data from the Aspen HYSYS® simulation violates the constraints, a penalty is imposed. The modified variables based on the fitness evaluation are returned to Aspen HYSYS®, and the thermodynamic properties are recalculated. This procedure is repeated until stopping criteria are satisfied, as illustrated in Figure 4.

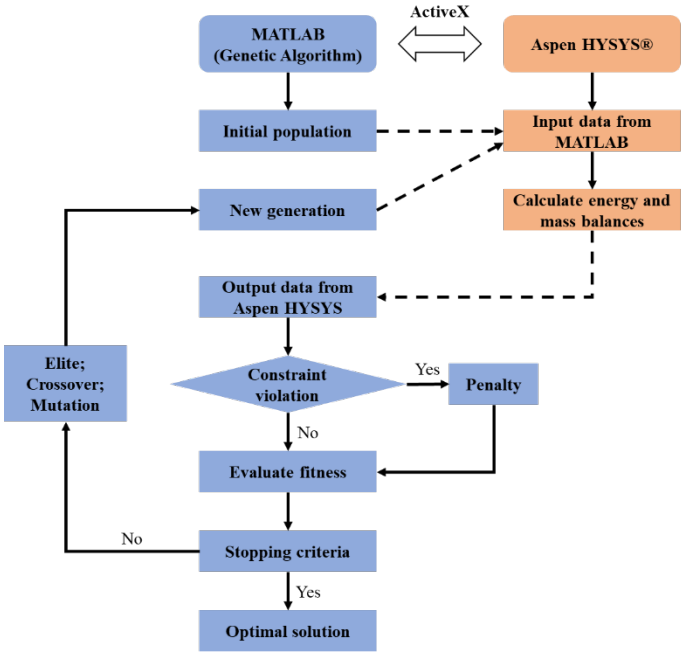

Figure 4. Optimization procedure

3.1. Cost estimation

For techno-economic optimization, the selection of a method for cost estimation must be considered. According to Symister [44], there are two alternative methods that can be used to estimate the cost of process systems: the module costing technique by Turton et al. [45] and the factorial costing technique by Towler and Sinnott [46]. The two techniques use different cost estimation factors. Symister [44] compared the two estimation methods and found that whereas the module costing technique has the advantage of handling more equipment types, the factorial costing technique is easier to apply. In this study, a modified version of the module costing technique was applied to estimate total annualized cost (TAC) of natural gas liquefaction processes while applying different types of MCHEs.

The procedure for calculating the TAC in this study, including the capital expenditures (CAPEX) and the operating expenditures (OPEX), is shown in Figure 5. Because the capacity applicable through the module costing technique is smaller than the target capacity of this study, the cost is first calculated for a base capacity (P_{base} = 0.16 MTPA). MTPA stands for million tonnes per annum. The sixth-tenths rule is then applied to account for the economy of scale when calculating the cost for the target capacity

(P_{target} = 1 MTPA). First, the purchased equipment cost (C_{p}^{0}) is calculated based on base-capacity equipment size with cost parameters (K_i) and the capacities of the equipment (A, e.g. power for compressors and expanders, area for MCHEs and coolers) as shown in Figure 5. Table 3 shows the types of equipment used and the cost parameters. The cost parameters (K_1, K_2 and K_3) are the correlation data for estimating the purchased equipment cost. The purchased equipment cost is based on the most common materials (carbon steel) and operation near atmospheric pressure. The bare module cost (C_{BM}), including direct expenses (such as the material cost required for the installation) and indirect expenses (such as the construction overhead), is calculated by applying a bare module factor (F_{BM}). Further, a total module cost factor (F_{TM}) is used to account for contingencies and fees in the total module cost (C_{TM}). The grassroots cost (C_{GR}), which covers the cost of auxiliary facilities, is calculated with a total module cost factor (F_{TM}), a grassroots cost factor (F_{GR}) and the bare module cost for base conditions (C_{BM}^{0}), as shown in Figure 5.

Because the equipment cost used in the estimation formula is based on historic data, it needs to be modified to reflect the time value. The time value of money is examined using the Chemical Engineering Plant Cost Index (CEPCI) [47] to adjust the cost of equipment in 2001, which is available in the literature [45], to the value of the target year using 2001 CEPCI (CI_{ref}) and 2017 CEPCI (CI_{target}). Consequently, CAPEX ($C_{\text{CAPEX}_{\text{base}}}$) can be calculated for the base capacity (P_{base}) as shown in Figure 5, where j is each piece of equipment, before CAPEX (C_{CAPEX}) for the target capacity (P_{target}) is estimated with the six-tenths rule.

OPEX ($C_{\text{OPEX}_{\text{base}}}$) is calculated for the base capacity first based on the net annual power consumption ($\dot{W}_{\text{total}}$) for the compressors and expanders and the annual cooling water supply ($\dot{Q}_{\text{cw}}$), and then OPEX (C_{OPEX}) for target capacity is calculated. The electricity cost (c_{elec}) and the cooling water supply cost (c_{cw}) are specified as 16.667 USD/GJ and 0.354 USD/GJ, respectively, according to Turton et al. [45]. When calculating the utility costs, the plant availability is assumed to be 93%. Labor and maintenance cost have not been included in the operating cost for this study.

CAPEX can be converted into annual capital expenditures (C_{CAPEX}) by considering the interest rate (i) and the lifetime of the plant (L). The interest rate and the lifetime of the plant are assumed to be 10% and 20 years, respectively. Finally, TAC can be calculated as the sum of the annualized capital cost and the operating cost.

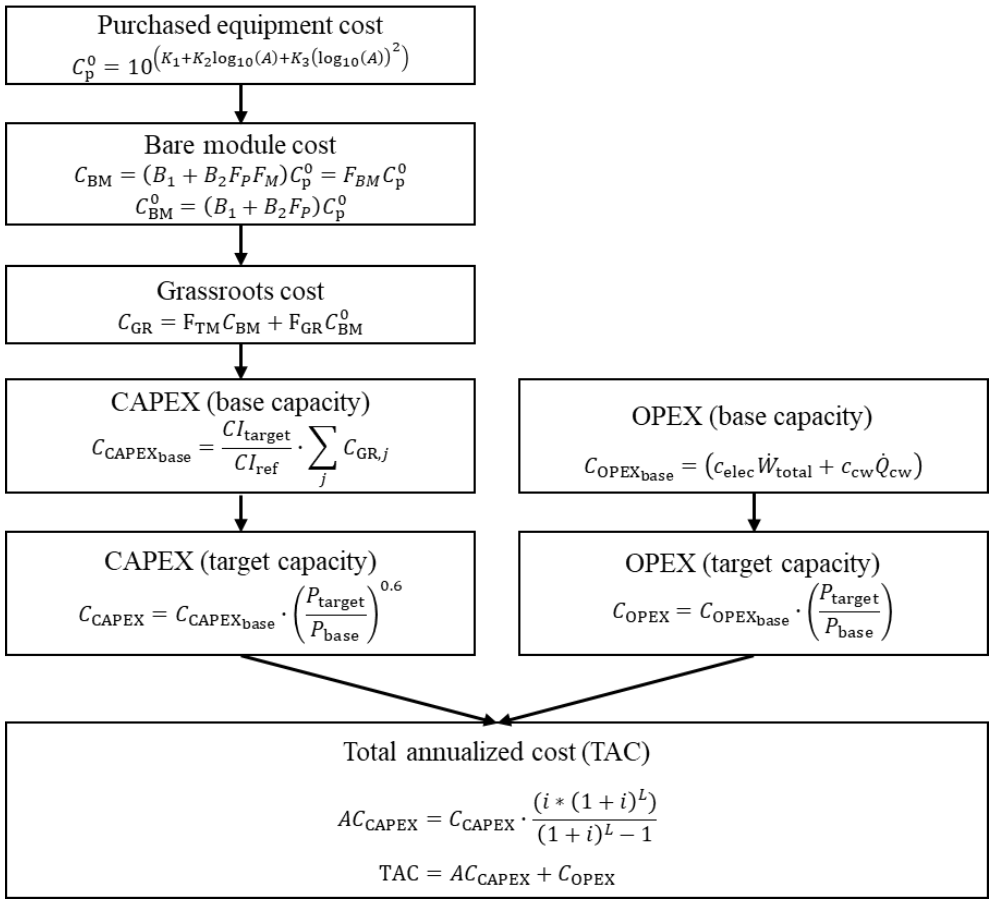

Figure 5. Calculation procedure for TAC [45]

Table 3. Types and cost parameters for each equipment [45]

Equipment	Type	C_{p}^{0}		
		K_1	K_2	K_3
MCHE	Flat plate (FPHE)	4.6656	-0.1557	0.1547
	Spiral tube (STHE)	3.9912	0.0668	0.243
Compressor	Centrifugal	2.2897	1.3604	-0.1027

Cooler	U-tube	4.1884	-0.2503	0.1974
Expander	Axial gas turbines	2.7051	1.4398	-0.1776

In this study, two types of MCHEs are applied in the cost estimation, a flat plate heat exchanger (FPHE) and a spiral tube heat exchanger (STHE), for which data are available from Turton et al. [45]. The STHE has a steeper cost increase per heat exchanger area than the FPHE, as can be observed from the cost parameters shown in Table 3. This indicates that STHEs and FPHEs can be regarded as high-cost heat exchangers and low-cost heat exchangers, respectively. In addition, it is assumed that the STHE has better heat transfer performance than the FPHE. The heat transfer rate is given by Eq. 1, where U is the overall heat transfer coefficient, A is the surface area available for heat transfer and ΔT_{LM} is the weighted logarithmic mean temperature difference (*LMTD*). Typically, the *U* value of the MCHE ranges from 1200 to 6000 W/m^2·°C according to previously published results [22, 48, 49]. In order to reflect the characteristics of the two different MCHEs in this study, the *U* values for one with relatively high heat transfer performance and the other with low heat transfer performance were assumed to be 5000 and 3000 W/m^2·°C, respectively. In addition, the sensitivity analysis was performed to accommodate the uncertainty in the *U* values, the results of which are described in Section 4.2 of the manuscript. The *U* values of the coolers were assumed to be 500 W/m^2·°C [30, 50].

$$\dot{\boldsymbol{Q}} = \boldsymbol{UA\Delta T_{\mathrm{LM}}} \tag{1}$$

3.2. Process optimization

In this study, two types of objective functions are selected. For the energy optimization, total power consumption is minimized:

$$\min \dot{\boldsymbol{W}}_{\mathbf{total}} = \sum_{i} \dot{\boldsymbol{W}}_{i} - \sum_{j} \dot{\boldsymbol{W}}_{j} \tag{2}$$

Here, $\dot{W}_i$ is the power consumed in the i^{th} compressor stage and $\dot{W}_j$ is the power produced in the j^{th} expander stage. The latter only applies to the dual expander process. For the techno-economic optimization, TAC (as defined in Figure 5) is minimized:

$$\mathbf{min}\ \boldsymbol{TAC} = \boldsymbol{AC}_{\mathbf{CAPEX}} + \boldsymbol{C}_{\mathbf{OPEX}} \tag{3}$$

In total, 13, 9, and 14 optimization variables were selected for the dual expander, SMR, and DMR processes, respectively, as shown in Table 4. In case of the DMR process, two temperature variables (hot stream temperatures after MCHE-1 and MCHE-2) were excluded from the set of optimization variables, for fast convergence during optimization, by specifying appropriate values for these variables as mentioned in Section 2.3. Multiple searches were performed in advance, and then the variable bounds presented in Table 4, which are the search limits of the variables suitable for the models in consideration, were selected as constraints to search for feasible solutions as much as possible during the optimization.

Table 4. Optimization variables and variable bounds for each process

Process	Variables	Stream	Lower bound	Upper bound
Dual expander	Pressure of N_2 refrigerant cycle (bar)	3	5	13
		5	13	25
		7	25	40
		9	40	80
		11	80	130
	Pressure of C_1 refrigerant cycle (bar)	14	15	25
		16	30	50
		18	60	90
		20	90	120
	Mass flow of N_2 refrigerant cycle (ton/h)	1	50	70
	Mass flow of C_1 refrigerant cycle (ton/h)	12	40	60
	Temperature of N_2 refrigerant cycle (℃)	2	-70	-40
	Temperature of C_1 refrigerant cycle (℃)	13	-10	10
SMR	Pressure (bar)	3	2.5	5
		5	5	10
		7	20	30
		N_2	5	15

	MR component flow rate (ton/h)	C_1	10	20
		C_2	30	50
		C_3	1	15
		n-C_4	5	20
		i-C_5	20	50
DMR	Pressure of WMR cycle (bar)	11	2.5	5
		2	5	10
		8	15	30
	Pressure of CMR cycle (bar)	23	2	5
		13	10	18
		15	18	30
		17	40	55
	WMR component flow rate (ton/h)	WMR_C_2	10	20
		WMR_C_3	1	5
		WMR_*n*-C_4	25	40
	CMR component flow rate (ton/h)	CMR_N_2	1	10
		CMR_C_1	5	20
		CMR_C_2	5	25
		CMR_C_3	5	25

In addition, equality and inequality constraints are set in Eqs. 4–7 to account for practical equipment limitations. MCHEs in natural gas liquefaction processes are mainly multi-stream heat exchangers and may provide high flexibility in the flow arrangement while minimizing the heat transfer area. Therefore, MCHEs may offer large heat transfer rates at temperature differences as small as 1–3 °C [51]. For energy optimization, therefore, results are obtained when the *MTA* constraint equal to 1, 2 and 3 °C, respectively, as given in Eq. 4, where MTA_k is the minimum temperature approach for the k^{th} MCHE. For techno-economic optimization, however, heat exchanger cost is considered in the objective function, and the use of an economic trade-off parameter is not required. Hence, the *MTA* constraint is only used as a practical limit with value 1 °C, as given in Eq. 5. In addition, in order to prevent liquid entering compressors, a constraint on the vapor fraction in the compressor inlet is used, as given by Eq. 6 where vf_i is the inlet vapor fraction for the i^{th} compressor stage. A constraint on maximum compression ratio is also used, as in Eq. 7 where p_i^{out} and p_i^{in} are the discharge and inlet pressures for the i^{th} compressor stage, respectively, owing to the technical limitations of compressors [52].

$$\boldsymbol{MTA_k \geq MTA_{limit} = 1, 2 \text{ or } 3\ ^\circ\text{C}\ \text{ (for energy optimization)}} \tag{4}$$

$$\boldsymbol{MTA_k \geq MTA_{limit} = 1\ ^{\circ}C\ \text{(for techno-economic optimization)}} \quad (5)$$

$$\boldsymbol{vf_i = 1} \quad (6)$$

$$\boldsymbol{p_i^{out}/p_i^{in} \leq 4} \quad (7)$$

3.3. Sensitivity analyses

Sensitivity analyses for *U* values and *MTA* constraints were performed for the SMR process as a representative case to further investigate the influence of the heat exchanger cost on the trade-off between energy efficiency and heat exchanger size.

The heat transfer area is inversely proportional to the *U* value, which strongly affects the heat exchanger cost. Because the *U* value of the MCHE is estimated to be 1200–6000 W/m^{2}·°C, as mentioned previously, sensitivity analysis was performed for *U* values of 2000, 3000, 4000, 5000 and 6000 W/m^{2}·°C.

To check the validity of the results from energy optimization, a sensitivity analysis of the value for this trade-off parameter (the *MTA* constraint) has been performed using the values 1, 2 and 3 °C for the *MTA*, as mentioned in Section 3.2.

4. Results

4.1. Results from energy and techno-economic optimization

When using power consumption as an objective function, the electricity cost can be minimized by reducing the compressor duties. In addition, as the compressor cost is a function of the compression power, reduced power consumption also leads to a reduction in the compressor cost. These savings should be compared with the increase in heat exchanger cost as the required total heat transfer area increases. This trade-off is the motivation for the introduction of techno-economic optimization. The

results of the energy and techno-economic optimizations for the dual expander, SMR, and DMR processes are shown in Tables 5–7.

For convenience, E1, E2, and E3 indicate energy optimization results with *MTA* constraints of 1, 2 and 3 °C, respectively. For the techno-economic optimization, results for the FPHE and STHE cases were obtained separately. TACs and SECs for each optimization result are shown in Figure 6. The capital cost, including the MCHE, compressor, cooler and expander costs, and the operating cost (the utility cost) are presented as cumulative bar charts. The separator, valve, pump, and mixer costs were negligible compared to the other equipment costs; therefore, they were excluded from the capital cost. Figure 7 presents the temperature differences throughout the MCHEs of each process optimization result to compare the obtained solutions. Here, the *MTA* constraints ($MTA \geq 1$, 2 or 3 °C) for energy optimization stand for MTA_{limit} in Eq. 4.

In the case of the energy optimization results of the dual expander process, as the *MTA* constraint value is reduced from 3 °C to 1 °C, the composite curves are more closely matched; thereby, the irreversibility of the MCHE is reduced, which can result in an increase in process efficiency. Considering the techno-economic optimization results of the dual expander process for both FPHE and STHE cases, process efficiencies similar to that of E1 were obtained. Owing to the relatively low process efficiency of the dual expander process, the utility and compressor costs have a significant influence on the TAC. Therefore, as shown in Figures 6(a) and 6(b), it is advantageous from an economic point of view to reduce the utility and compressor costs by increasing the process efficiency. Because the area of the MCHE required for the dual expander process at a given constant *U* value is smaller than that of the MR process, the MCHE cost has no significant influence on the TAC. As a result, the solution for the techno-economic optimization of the dual expander process is shifted towards high process efficiency, similar to the energy optimization. As shown in Figure 7(a), the energy optimization and the techno-economic optimization provide similar temperature profiles in the MCHE, indicating that similar solutions have been obtained.

Figures 6(c) and 6(d) show the TAC results when FPHE and STHE, respectively, are applied in the

SMR process. The utility and compressor costs of the SMR process are lower than those of the dual-expander process owing to the relatively high process efficiency. In combination with increased heat duty, reduced driving forces in the MCHE also leads to increased *UA* value, and thereby increased MCHE cost. Considering the FPHE case in Figure 6(c), the energy optimization reduces TAC as the *MTA* constraint value is reduced from 3 °C to 2 °C, reducing the utility cost. However, TAC is increased as the *MTA* constraint value is reduced from 2 °C to 1 °C, as the effect of increased MCHE cost is stronger than the effect of reduced utility cost. For the STHE case in Figure 6(d), E3 provides the lowest TAC among the energy optimization results as the unit cost of MCHE increases. The results of the techno-economic optimization provide solutions with lower TACs even though the SECs are higher. This proves that the techno-economic optimization found a better trade-off between process efficiency and MCHE cost. For the FPHE case, the techno-economic optimization reduces the TAC by 5.7%, 3.2%, and 5.8% compared to E1, E2, and E3, respectively. For the STHE case, the techno-economic optimization reduces the TAC by 22.8%, 13.8%, and 8.4% compared to E1, E2, and E3, respectively, by significantly reducing the MCHE cost. Notably, as shown in Table 6, the *UA* value of the techno-economic optimization for the FPHE case is lower than that of the E2 even though the SECs are similar. The techno-economic optimization resulted in a better distribution of temperature driving forces in the MCHE compared to the energy optimization because the techno-economic optimization can evaluate whether the MCHE cost and size are appropriate values in terms of TAC, thereby avoiding unnecessary increase in the MCHE size. According to Austbø and Gundersen [53, 54], the optimal distribution of the temperature driving forces in a low-temperature process can be obtained when the temperature driving forces are proportional to the temperature level. As shown in Figure 7(b), the temperature differences of the techno-economic optimization are more proportional to the temperature level than the one from the energy optimization. This aspect is also observed in the dual expander process and the DMR process.

The DMR process has a high energy efficiency, resulting in a low utility cost, as shown in Figure 6(e) and 6(f). Considering the FPHE case in Figure 6(e), because of the small contribution from the heat exchanger cost, the solution of the techno-economic optimization is obtained such that the operating

cost is minimized, similar to the energy optimization. In the case of the STHE, however, a solution with smaller MCHE is favorable despite the accompanying higher utility cost. Figure 6(f) illustrates these results in the sense that the techno-economic optimization with STHE reduces the TAC by 14.5%, 6.6%, and 3.4% compared to E1, E2, and E3, respectively. The weighted logarithmic mean temperature difference in the techno-economic optimization with STHE is larger than those of E1, E2 and E3, as well as the FPHE case, as shown in Figure 7(c). This clearly shows that the optimal solution from techno-economic optimization of a liquefaction process can be quite far away from the results obtained when using energy optimization of the same process, when the contribution from the heat exchanger cost is significant in the TAC.

Table 5. Optimization results for the dual expander process

Item	Stream	Unit	Energy optimization			Techno-economic optimization	
			E3 (MTA_{limit} = 3 ℃)	E2 (MTA_{limit} = 2 ℃)	E1 (MTA_{limit} = 1 ℃)	FPHE	STHE
N_2 pressure	3	bar	10.1	10.9	10.6	10.4	11.1
	5		20.1	21.4	21.0	21.3	21.9
	7		34.4	37.8	36.9	37.4	36.8
	9		60.9	66.0	64.4	65.0	61.3
	11		111.2	113.8	111.0	112.2	101.4
C_1 pressure	14	bar	24.1	23.5	25.0	24.9	25.0
	16		42.4	40.0	42.1	43.7	42.9
	18		67.2	64.9	68.4	71.8	69.2
	20		106.9	102.0	108.1	115.1	108.9
N_2 mass flow	1	ton/h	63.9	63.1	63.3	63.0	61.4
C_1 mass flow	12	ton/h	55.3	55.9	54.0	51.2	58.6
N_2 temperature after MCHE	2	℃	-64.4	-64.7	-63.6	-62.2	-69.8

C_1 temperature after MCHE	13	℃	7.1	6.5	7.6	8.5	0.7
SEC	-	kWh/ton LNG	365.1	357.7	351.5	353.5	352.1
TAC	-	MUSD/ year	32.3 (FPHE) 33.1 (STHE)	31.9 (FPHE) 33.1 (STHE)	31.6 (FPHE) 33.2 (STHE)	31.6	32.2
UA	MCHE-1	kW/℃	1172	1529	2016	1533	1289
Heat duty		kW	7344	7362	7257	7138	7785
LMTD		℃	6.3	4.8	3.6	4.7	6.0
MTA_k		℃	3.0	2.0	1.0	1.0	1.0

Table 6. Optimization results for the SMR process

Variable	Stream	Unit	Energy optimization			Techno-economic optimization	
			E3 (MTA_{limit} = 3 ℃)	E2 (MTA_{limit} = 2 ℃)	E1 (MTA_{limit} = 1 ℃)	FPHE	STHE
MR pressure	3	bar	3.9	4.4	4.8	3.9	2.8
	5		6.4	7.0	7.2	6.7	6.3
	7		21.5	20.7	22.8	23.0	23.0
MR Composition	N_2	ton/h	10.1	9.4	8.7	7.4	6.3
	C_1		13.0	14.5	13.0	12.5	10.7
	C_2		38.7	36.0	38.3	33.5	30.2
	C_3		9.3	10.0	4.8	7.5	6.6
	n-C_4		8.7	17.9	20.0	15.9	16.2
	i-C_5		33.1	25.9	22.8	23.9	22.8
SEC	-	kWh/ton LNG	266.6	242.3	230.5	245.6	268.4
TAC	-	MUSD/year	21.0 (FPHE) 25.0 (STHE)	20.5 (FPHE) 26.5 (STHE)	21.0 (FPHE) 29.7 (STHE)	19.8	22.9
UA		kW/℃	5021	7719	10963	5998	3428

Heat duty	MCHE-1	kW	22323	22746	21597	20286	18675
LMTD		℃	4.4	2.9	2.0	3.4	5.4
MTA_k		℃	3.0	2.0	1.0	1.1	2.2

Table 7. Optimization results for the DMR process

Variable	Stream	Unit	Energy optimization			Techno-economic optimization	
			E3 (MTA_{limit} = 3 ℃)	E2 (MTA_{limit} = 2 ℃)	E1 (MTA_{limit} = 1 ℃)	FPHE	STHE
Precooling MR pressure	7	bar	3.3	4.0	3.8	3.0	3.6
	2		7.9	9.0	8.7	7.7	9.5
	4		15.7	17.8	17.2	15.4	19.1
Main cryogenic MR pressure	19	bar	3.0	3.4	3.3	3.1	3.1
	9		12.0	13.8	13.0	12.4	12.4
	11		25.0	26.7	24.0	24.3	26.0
	13		47.4	47.8	41.2	42.2	47.5
Precooling MR composition	C_2	ton/h	13.0	15.1	14.2	10.8	15.1
	C_3		5.6	5.5	5.8	8.0	6.5
	n-C_4		31.6	29.0	30.0	27.9	25.4
Main cryogenic MR composition	N_2	ton/h	2.8	3.0	2.3	2.3	2.5
	C_1		10.0	10.0	10.0	9.1	9.7
	C_2		12.5	13.3	13.0	14.0	14.0
	C_3		14.0	13.3	14.0	12.8	11.9
SEC	-	kWh/ton LNG	242.9	232.6	225.3	227.1	244.9
TAC	-	MUSD/ year	20.1 (FPHE) 22.0 (STHE)	19.8 (FPHE) 22.7 (STHE)	20.0 (FPHE) 24.8 (STHE)	19.3	21.2
UA	MCHE-1	kW/℃	1466	2122	3160	1568	896
	MCHE-2		1288	1762	2793	2206	1154
	MCHE-3		153	211	303	291	244

Heat duty	MCHE-1	kW	6718	6695	6731	6479	6445
	MCHE-2		5917	5955	6045	5854	5841
	MCHE-3		769	775	798	758	752
LMTD	MCHE-1	℃	4.6	3.2	2.1	4.1	7.2
	MCHE-2		4.6	3.4	2.2	2.7	5.1
	MCHE-3		5.0	3.7	2.6	2.6	3.1
MTA_k	MCHE-1	℃	3.0	2.0	1.0	2.2	5.8
	MCHE-2		3.0	2.0	1.0	1.2	1.0
	MCHE-3		3.1	2.0	1.1	1.2	1.6

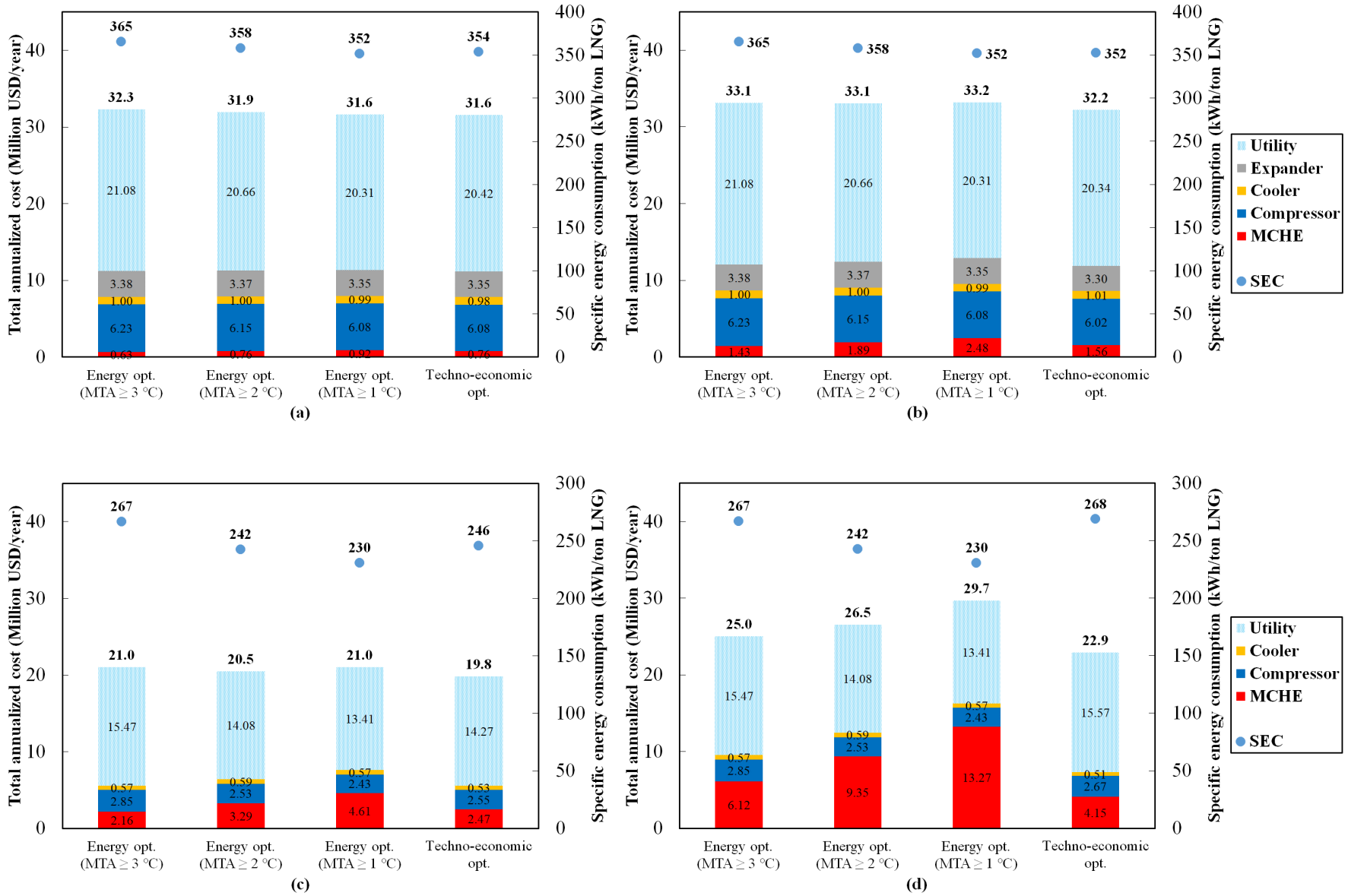
Total annualized cost (Million USD/year)
Specific energy consumption (kWh/ton LNG)
Energy opt. (MTA ≥ 3 °C)
Energy opt. (MTA ≥ 2 °C)
Energy opt. (MTA ≥ 1 °C)
Techno-economic opt.
(a)
365
358
352
354
32.3
31.9
31.6
31.6
21.08
20.66
20.31
20.42
3.38
3.37
3.35
3.35
1.00
1.00
0.99
0.98
6.23
6.15
6.08
6.08
0.63
0.76
0.92
0.76
(b)
365
358
352
352
33.1
33.1
33.2
32.2
21.08
20.66
20.31
20.34
3.38
3.37
3.35
3.30
1.00
1.00
0.99
1.01
6.23
6.15
6.08
6.02
1.43
1.89
2.48
1.56
(c)
267
242
230
246
21.0
20.5
21.0
19.8
15.47
14.08
13.41
14.27
0.57
0.59
0.57
0.53
2.85
2.53
2.43
2.55
2.16
3.29
4.61
2.47
(d)
267
242
230
268
25.0
26.5
29.7
22.9
15.47
14.08
13.41
15.57
0.57
0.59
0.57
0.51
2.85
2.53
2.43
2.67
6.12
9.35
13.27
4.15
Utility
Expander
Cooler
Compressor
MCHE
SEC

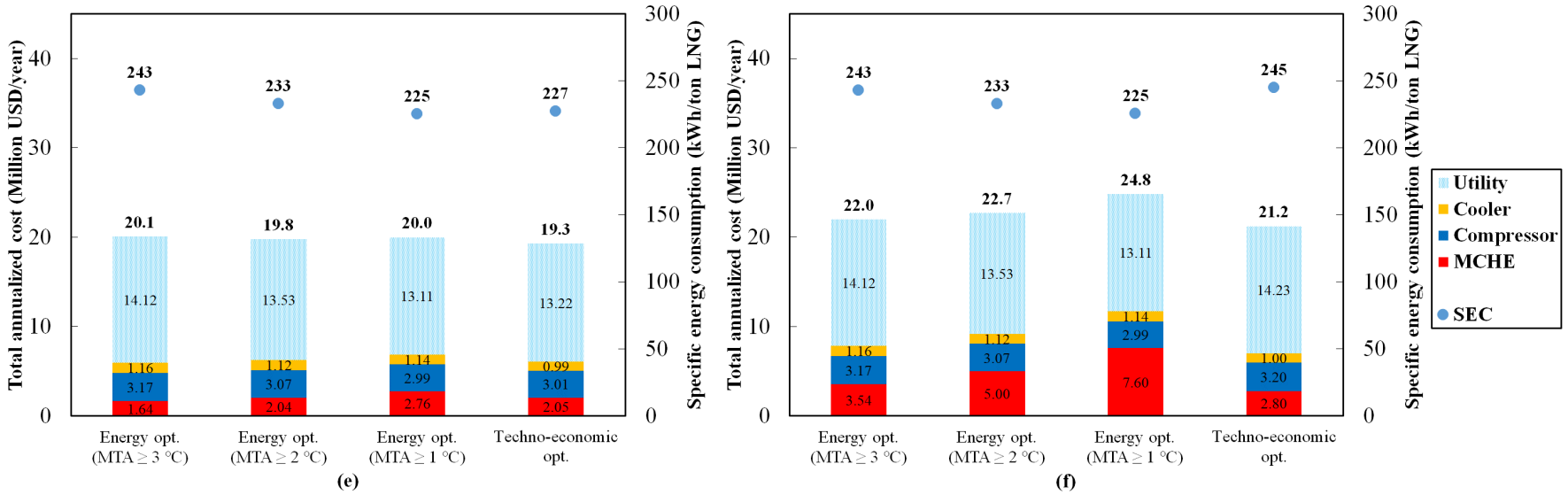

Figure 6. Total Annualized Cost, including CAPEX and OPEX, and SEC for each optimization case: (a) Dual expander process with FPHE, (b) Dual expander process with STHE, (c) SMR process with FPHE, (d) SMR process with STHE, (e) DMR process with FPHE, and (f) DMR process with STHE

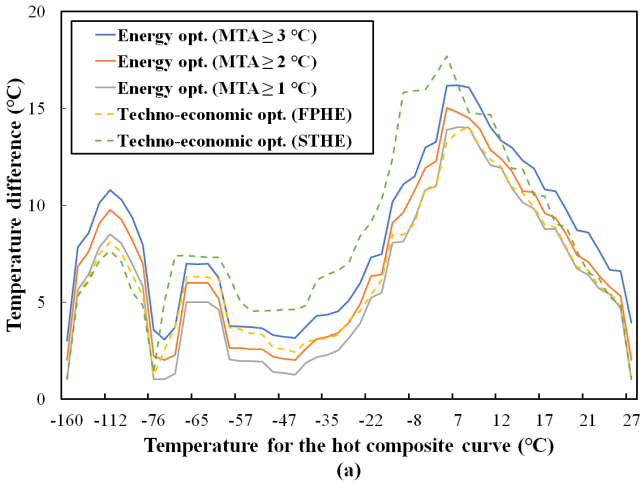

(a)

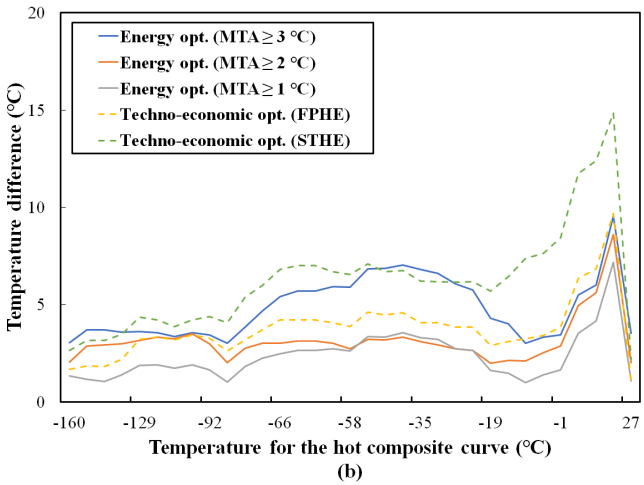

(b)

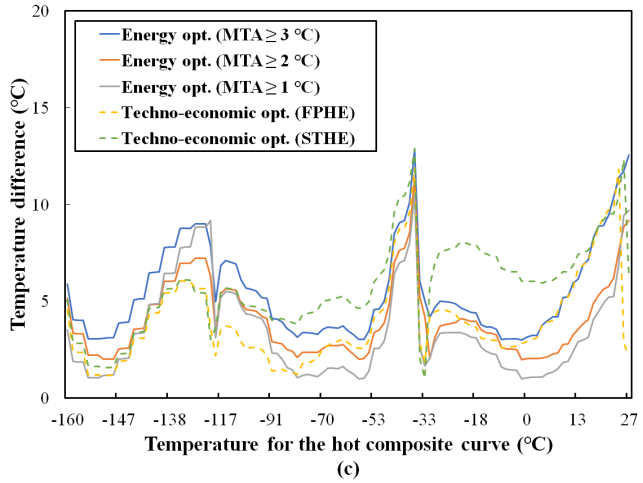

(c)

Figure 7. Temperature differences for each process: (a) Dual expander process, (b) SMR process, and (c) DMR process

4.2. Sensitivity analyses

Sensitivity analyses for *U* values and *MTA* constraints were performed for the SMR process to investigate how *U* values and MCHE cost influence the *MTA* constraint as an economic trade-off parameter. Figures 8(a) and 8(b) show the TAC results as a function of the *MTA* constraint value for different *U* values when FPHE and STHE are applied, respectively. Since the *MTA* constraint is not applied as an economic trade-off parameter in the techno-economic optimization, the TAC is independent of the *MTA* value. The TACs of the energy optimization, however, have different values depending on the *MTA* constraint.

In the case of FPHE with high *U* value, it can be seen that the TAC differences between energy and techno-economic optimizations are relatively small because of the minor contribution of the MCHE cost to TAC. However, the difference tends to increase when the *U* value decreases, since this leads to larger MCHE areas and thereby higher MCHE cost. The smaller the *U* value, the larger the optimal *MTA* value (providing the smallest TAC for the energy optimization). In the case of STHE, the trend is similar to that of the FPHE case, but the optimal *MTA*s for the energy optimization have higher values and the differences in TAC between the results from the techno-economic optimization and the energy optimization are larger because of the high unit cost of the MCHE.

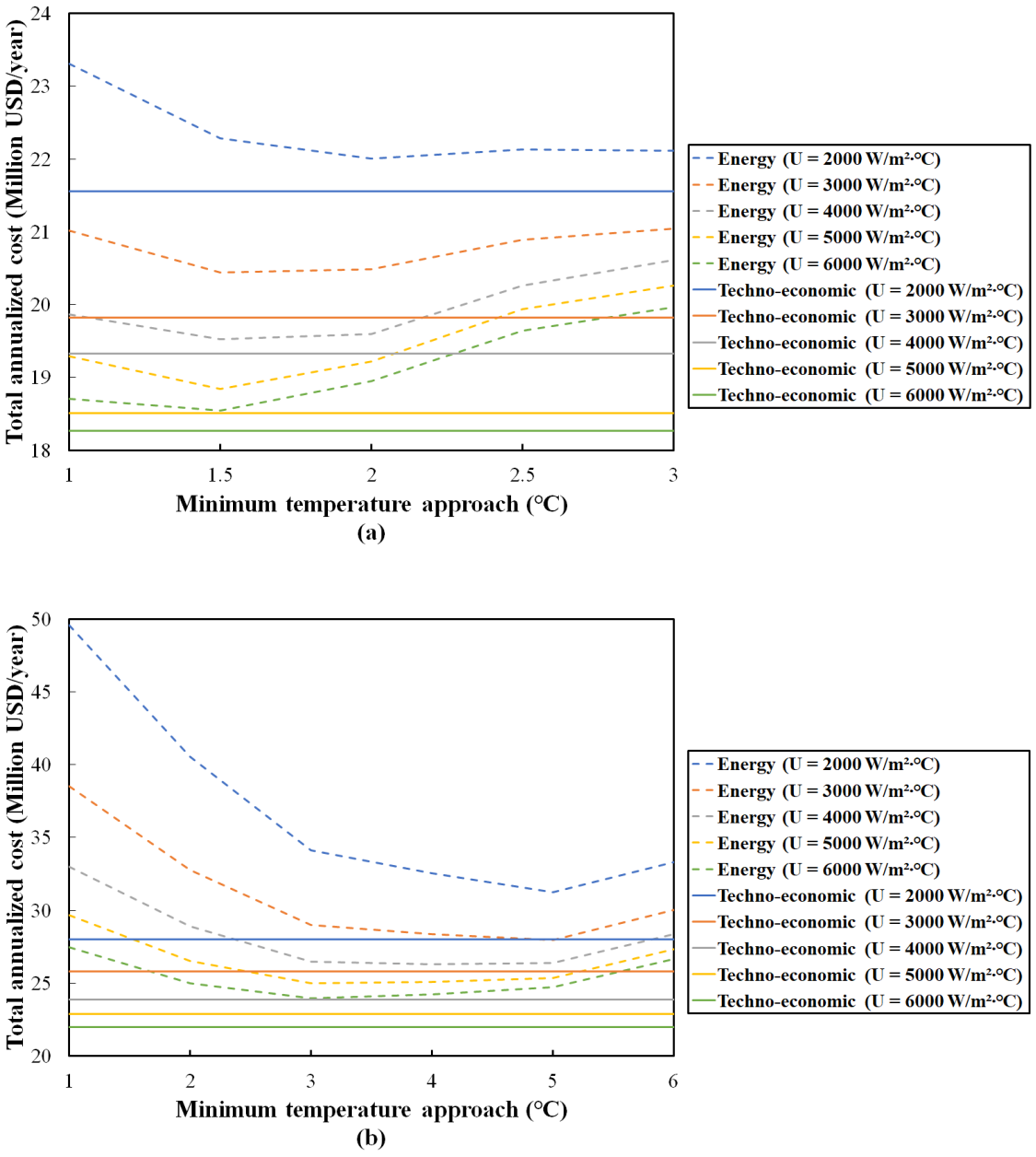

Figure 8. TAC results as a function of the *MTA* constraint with the different *U* values: (a) FPHE case and (b) STHE case

5. Discussion

In order to examine the results of this study, several limitations should be considered. One important limitation is the accuracy of the cost estimation method applied. Because it is difficult to obtain detailed vendor data, a commonly used approach for estimating the cost of a chemical process is applied in this study. Unfortunately, this method is not very accurate for the equipment in natural gas liquefaction

processes. Another limitation is the heat exchanger model used in this study, which assumes constant U values. In addition, the heat exchanger area is calculated based on composite curves, assuming countercurrent flow. Therefore, the assumed U values can affect the size and thereby cost of the MCHEs. Future work should include the application of more accurate cost estimation methods and more detailed heat exchanger models. In addition, the pressure drops of MCHEs and coolers are neglected in this study. If the pressure drop is considered, the resulting values will be slightly different as the power consumed in the liquefaction process increases. However, the trend in the comparisons is not expected to change significantly.

6. Conclusion

Techno-economic optimization was applied to three liquefaction processes (i.e. dual expander, SMR and DMR) and was performed for two different MCHE types with different unit cost and heat transfer performance. The results were compared to those obtained using energy optimization. In addition, appropriate values for *MTA* constraints as economic trade-off parameters in energy optimization were investigated. The following are important results of this study:

1) Techno-economic optimization can provide a better distribution of temperature driving forces in the MCHE because the MCHE cost can be assessed and an unprofitable increase in the MCHE size can be avoided during the optimization.

2) Energy optimization performs better for low-efficiency processes than high-efficiency processes in terms of TAC because the MCHE cost is of less importance.

    - For the dual expander process with relatively low energy efficiency, the operating and compressor capital costs have a significant influence on the TAC. Therefore, it is advantageous from an economic point of view to reduce the operating cost by increasing the process efficiency. In contrast, for MR processes with relatively high energy efficiency, the influence of the MCHE cost on the TAC increases. Therefore, the MCHE cost increase due to increase

in energy efficiency can be a worse case from an economic point of view, and therefore the trade-off between the MCHE cost and energy efficiency should be closely investigated.

3) A reduced *MTA* constraint value in energy optimization is advantageous in terms of process efficiency, but it can be detrimental in terms of TAC, and therefore it is important to use an appropriate value for the *MTA* constraint depending on the process characteristics.

4) The proper value for the *MTA* constraint in energy optimization increases with increased MCHE unit cost and reduced *U* values because the optimal economic trade-off is shifted towards smaller MCHEs.

The results indicate that it is sufficient to use energy optimization to design expander liquefaction processes. However, it is better to apply techno-economic optimization than energy optimization if MR liquefaction processes are designed, especially when an MCHE with a high unit cost is installed. Nevertheless, a good solution in terms of cost can be obtained in energy optimization if an appropriate value for the *MTA* constraint as an economic trade-off parameter is selected.

As potential future research, a study on cost estimation methods with added cost factors for safety, a techno-economic optimization study for offshore platforms, where size and footprint become more important factors in process design, and a study for the application of a more accurate heat exchanger model may be conducted.

Acknowledgments

Funding:

This research was supported by the MOTIE (Ministry of Trade, Industry, and Energy) in Korea, under the Fostering Global Talents for Innovative Growth Program (P0008747) supervised by the Korea Institute for Advancement of Technology (KIAT).

This work was supported by the National Research Foundation of Korea (NRF) grant funded by the Korea government (MSIT) (No. 2021M3H7A102621612).

Nomenclature

Abbreviation

CAPEX	capital expenditures
CEPCI	chemical engineering plant cost index
CMR	cold mixed refrigerant
C_3MR	propane precooled mixed refrigerant
DMR	dual mixed refrigerant
E1	Energy optimization with the *MTA* constraint ($MTA \geq 1$ ℃)
E2	Energy optimization with the *MTA* constraint ($MTA \geq 2$ ℃)
E3	Energy optimization with the *MTA* constraint ($MTA \geq 3$ ℃)
FPHE	flat plate heat exchanger
GA	genetic algorithm
LMTD	logarithmic mean temperature difference
LNG	liquefied natural gas
MCHE	main cryogenic heat exchanger
MINLP	mixed-integer non-linear programming
MR	mixed refrigerant
MTA	minimum temperature approach
NG	natural gas
NPV	net present value
OPEX	operating expenditures
SEC	specific energy consumption
SMR	single mixed refrigerant
SQP	sequential quadratic programming
STHE	spiral tube heat exchanger
TAC	total annualized cost
WMR	warm mixed refrigerant

Symbols

N_2	nitrogen
C_1	methane
C_2	ethane
C_3	propane

C_4	butane
i-C_4	isobutane
n-C_4	normal butane
i-C_5	isopentane
P_{base}	base capacity, MTPA
P_{target}	target capacity, MTPA
C_{p}^{0}	purchased equipment cost, USD
K_i	cost parameter
C_{BM}	bare module cost, USD
C_{BM}^{0}	bare module cost for base conditions, USD
B_i	constants for bare module factor
F_P	pressure factor
F_M	material factor
F_{BM}	bare module factor
C_{TM}	total module cost, USD
F_{TM}	total module factor
C_{GR}	grassroots cost, USD
F_{GR}	grassroots cost factor
CI_{ref}	2001 CEPCI
CI_{target}	2017 CEPCI
$C_{\text{CAPEX}_{\text{base}}}$	base CAPEX for base capacity, USD
C_{CAPEX}	CAPEX for target capacity, USD
$\dot{W}_{\text{total}}$	net annual power consumption, kW
$\dot{Q}_{\text{cw}}$	annual cooling water supply, kW
c_{elec}	electricity cost, USD/GJ
c_{cw}	cooling water supply cost, USD/GJ
AC_{CAPEX}	annual CAPEX, USD/year
i	interest rate
L	lifetime of the plant
U	overall heat transfer coefficient, W/m^{2}·°C
$\dot{W}_i$	power consumed in the i^{th} compressor stage, kW
$\dot{W}_j$	power produced in the j^{th} expander stage, kW
MTA_k	minimum temperature approach for the k^{th} MCHE, ℃
MTA_{limit}	limitation on minimum temperature approach, ℃
vf_i	inlet vapor fraction for the i^{th} compressor stage
p_i^{out}	discharge pressure for the i^{th} compressor stage, bar
p_i^{in}	inlet pressure for the i^{th} compressor stage, bar

References

[1] X. Wang, M. Li, L. Cai, and Y. Li, "Propane and iso-butane pre-cooled mixed refrigerant liquefaction process for small-scale skid-mounted natural gas liquefaction," *Applied Energy,* vol. 275, p. 115333, 2020.

[2] S. Kumar *et al.*, "LNG: An eco-friendly cryogenic fuel for sustainable development," *Applied Energy,* vol. 88, no. 12, pp. 4264-4273, 2011.

[3] C. Hwang and Y. Lim, "Optimal process design of onboard BOG re-liquefaction system for LNG carrier," *Journal of Ocean Engineering and Technology,* vol. 32, no. 5, pp. 372-379, 2018.

[4] W. You, M. Chae, J. Park, and Y. Lim, "Potential explosion risk comparison between SMR and DMR liquefaction processes at conceptual design stage of FLNG," *Journal of Ocean Engineering and Technology,* vol. 32, no. 2, pp. 95-105, 2018.

[5] ExxonMobil, "Outlook for Energy: A Perspective to 2040," 2019.

[6] B. P. Center, "Annual Energy Outlook 2020," *Energy Information Administration, Washington, DC,* 2020.

[7] B. Austbø, S. W. Løvseth, and T. Gundersen, "Annotated bibliography—Use of optimization in LNG process design and operation," *Computers & Chemical Engineering,* vol. 71, pp. 391-414, 2014.

[8] P. E. Wahl, S. W. Løvseth, and M. J. Mølnvik, "Optimization of a simple LNG process using sequential quadratic programming," *Computers & Chemical Engineering,* vol. 56, pp. 27-36, 2013.

[9] A. Aspelund, T. Gundersen, J. Myklebust, M. Nowak, and A. Tomasgard, "An optimization-simulation model for a simple LNG process," *Computers & Chemical Engineering,* vol. 34, no. 10, pp. 1606-1617, 2010.

[10] A. Morin, P. E. Wahl, and M. Mølnvik, "Using evolutionary search to optimise the energy consumption for natural gas liquefaction," *Chemical Engineering Research and Design,* vol. 89, no. 11, pp. 2428-2441, 2011.

[11] A. Alabdulkarem, A. Mortazavi, Y. Hwang, R. Radermacher, and P. Rogers, "Optimization of propane pre-cooled mixed refrigerant LNG plant," *Applied Thermal Engineering,* vol. 31, no. 6-7, pp. 1091-1098, 2011.

[12] A. Mortazavi, C. Somers, A. Alabdulkarem, Y. Hwang, and R. Radermacher, "Enhancement of APCI cycle efficiency with absorption chillers," *Energy,* vol. 35, no. 9, pp. 3877-3882, 2010.

[13] M. M. H. Shirazi and D. Mowla, "Energy optimization for liquefaction process of natural gas in peak shaving plant," *Energy,* vol. 35, no. 7, pp. 2878-2885, 2010.

[14] J.-H. Hwang, M.-I. Roh, and K.-Y. Lee, "Determination of the optimal operating conditions of the dual mixed refrigerant cycle for the LNG FPSO topside liquefaction process," *Computers & Chemical Engineering,* vol. 49, pp. 25-36, 2013.

[15] M. J. Roberts and R. Agrawal, "Dual mixed refrigerant cycle for gas liquefaction," ed: Google Patents, 2001.

[16] G. Venkatarathnam and K. D. Timmerhaus, *Cryogenic mixed refrigerant processes*. Springer, 2008.

[17] M. Wang, J. Zhang, and Q. Xu, "Optimal design and operation of a C3MR refrigeration system for natural gas liquefaction," *Computers & Chemical Engineering,* vol. 39, pp. 84-95, 2012.

[18] M. S. Khan, S. Lee, G. Rangaiah, and M. Lee, "Knowledge based decision making method for the selection of mixed refrigerant systems for energy efficient LNG processes," *Applied Energy,* vol. 111, pp. 1018-1031, 2013.

[19] T. He and Y. Ju, "Optimal synthesis of expansion liquefaction cycle for distributed-scale LNG (liquefied natural gas) plant," *Energy,* vol. 88, pp. 268-280, 2015.

[20] M. A. Qyyum, K. Qadeer, S. Lee, and M. Lee, "Innovative propane-nitrogen two-phase expander refrigeration cycle for energy-efficient and low-global warming potential LNG production," *Applied Thermal Engineering,* vol. 139, pp. 157-165, 2018.

[21] H.-M. Chang, M. J. Chung, S. Lee, and K. H. Choe, "An efficient multi-stage Brayton–JT cycle for liquefaction of natural gas," *Cryogenics,* vol. 51, no. 6, pp. 278-286, 2011.

[22] M. A. Qyyum, T. He, K. Qadeer, N. Mao, S. Lee, and M. Lee, "Dual-effect single-mixed refrigeration cycle: An innovative alternative process for energy-efficient and cost-effective natural gas liquefaction," *Applied Energy,* vol. 268, p. 115022, 2020.

[23] M. Kanoglu, I. Dincer, and M. A. Rosen, "Performance analysis of gas liquefaction cycles," *International Journal of Energy Research,* vol. 32, no. 1, pp. 35-43, 2008.

[24] C. W. Remeljej and A. F. A. Hoadley, "An exergy analysis of small-scale liquefied natural gas (LNG) liquefaction processes," *Energy,* vol. 31, no. 12, pp. 2005-2019, 2006.

[25] E. Primabudi, "Evaluation and optimization of natural gas liquefaction process with exergy-based methods: a case study for C3MR," Doctoral Thesis, TU Berlin, Berlin, Germany, 2019.

[26] H.-M. Chang, "A thermodynamic review of cryogenic refrigeration cycles for liquefaction of natural gas," *Cryogenics,* vol. 72, pp. 127-147, 2015.
[27] M. N. Bin Omar, "Thermodynamic and economic evaluation of existing and prospective processes for liquefaction of natural gas in Malaysia," dissertation, TU Berlin, Berlin, Germany, 2016.
[28] F. J. Barnés and C. J. King, "Synthesis of cascade refrigeration and liquefaction systems," *Industrial & Engineering Chemistry Process Design and Development,* vol. 13, no. 4, pp. 421-433, 1974.
[29] F. Del Nogal, J.-K. Kim, S. Perry, and R. Smith, "Optimal design of mixed refrigerant cycles," *Industrial & Engineering Chemistry Research,* vol. 47, no. 22, pp. 8724-8740, 2008.
[30] J. B. Jensen and S. Skogestad, "Problems with Specifying ΔT min in the Design of Processes with Heat Exchangers," *Industrial & Engineering Chemistry Research,* vol. 47, no. 9, pp. 3071-3075, 2008.
[31] P. Hatcher, R. Khalilpour, and A. Abbas, "Optimisation of LNG mixed-refrigerant processes considering operation and design objectives," *Computers & Chemical Engineering,* vol. 41, pp. 123-133, 2012.
[32] M. Wang, R. Khalilpour, and A. Abbas, "Thermodynamic and economic optimization of LNG mixed refrigerant processes," *Energy Conversion and Management,* vol. 88, pp. 947-961, 2014.
[33] J. Zhang, H. Meerman, R. Benders, and A. Faaij, "Technical and economic optimization of expander-based small-scale natural gas liquefaction processes with absorption precooling cycle," *Energy,* vol. 191, p. 116592, 2020.
[34] D.-Y. Peng and D. B. Robinson, "A new two-constant equation of state," *Industrial & Engineering Chemistry Fundamentals,* vol. 15, no. 1, pp. 59-64, 1976.
[35] H. Paradowski and P. Hagyard, "Comparing five LNG processes," *Hydrocarbon Engineering,* vol. 8, no. 10, pp. 32-37, 2003.
[36] W. Lim, K. Choi, and I. Moon, "Current status and perspectives of liquefied natural gas (LNG) plant design," *Industrial & Engineering Chemistry Research,* vol. 52, no. 9, pp. 3065-3088, 2013.
[37] T. He, I. A. Karimi, and Y. Ju, "Review on the design and optimization of natural gas liquefaction processes for onshore and offshore applications," *Chemical Engineering Research and Design,* vol. 132, pp. 89-114, 2018.
[38] Q. Li and Y. Ju, "Design and analysis of liquefaction process for offshore associated gas resources," *Applied Thermal Engineering,* vol. 30, no. 16, pp. 2518-2525, 2010.
[39] M. S. Khan, S. Lee, M. Getu, and M. Lee, "Knowledge inspired investigation of selected parameters on energy consumption in nitrogen single and dual expander processes of natural gas liquefaction," *Journal of Natural Gas Science and Engineering,* vol. 23, pp. 324-337, 2015.
[40] M. Wang, J. Zhang, Q. Xu, and K. Li, "Thermodynamic-analysis-based energy consumption minimization for natural gas liquefaction," *Industrial & Engineering Chemistry Research,* vol. 50, no. 22, pp. 12630-12640, 2011.
[41] T. He, N. Mao, Z. Liu, M. A. Qyyum, M. Lee, and A. M. Pravez, "Impact of mixed refrigerant selection on energy and exergy performance of natural gas liquefaction processes," *Energy,* vol. 199, p. 117378, 2020.
[42] A. Mortazavi, C. Somers, Y. Hwang, R. Radermacher, P. Rodgers, and S. Al-Hashimi, "Performance enhancement of propane pre-cooled mixed refrigerant LNG plant," *Applied Energy,* vol. 93, pp. 125-131, 2012.
[43] M. Mitchell, *An introduction to genetic algorithms*. MIT press, 1998.
[44] O. J. Symister, "An analysis of capital cost estimation techniques for chemical processing," M.S. thesis, Chemical Engineering, Florida Institute of Technology, Melbourne, FL, USA, 2016.
[45] R. Turton, R. C. Bailie, W. B. Whiting, and J. A. Shaeiwitz, *Analysis, synthesis and design of chemical processes*. Pearson Education, 2008.
[46] G. Towler and R. Sinnott, *Chemical engineering design: principles, practice and economics of plant and process design*. Elsevier, 2012.
[47] M. P. Bailey, "Chemical engineering plant cost index (cepci)," *Chemical Engineering,* vol. 121, no. 2, pp. 68-69, 2014.
[48] P. S. O'Neill, C. F. Gottzmann, and J. W. Terbot, "Novel heat exchanger increases cascade cycle efficiency for natural gas liquefaction," in *Advances in Cryogenic Engineering*: Springer, 1972, pp. 420-437.
[49] S. Kakac, H. Liu, and A. Pramuanjaroenkij, *Heat exchangers: selection, rating, and thermal design*. CRC press, 2020.
[50] M. Stewart, *Surface Production Operations: Vol 2: Design of Gas-Handling Systems and Facilities*. Gulf Professional Publishing, 2014.
[51] M. F. Hasan, I. Karimi, H. Alfadala, and H. Grootjans, "Operational modeling of multistream heat exchangers with phase changes," *AIChE Journal,* vol. 55, no. 1, pp. 150-171, 2009.
[52] B. A. Finlayson, *Introduction to chemical engineering computing*. Wiley Online Library, 2006.

[53] B. Austbø and T. Gundersen, "Optimal distribution of temperature driving forces in low-temperature heat transfer," *AIChE Journal,* vol. 61, no. 8, pp. 2447-2455, 2015.
[54] B. Austbø and T. Gundersen, "Impact of problem formulation on LNG process optimization," *AIChE Journal,* vol. 62, no. 10, pp. 3598-3610, 2016.